Three-Dimensional Solutions to the Euler Equations with One Million Grid Points

Arthur Rizzi*
The Aeronautical Research Institute of Sweden
Bromma, Sweden

Introduction

THE accuracy of a computed solution to the Euler equations is related directly to the number of grid points that discretize the problem. Comparing a given solution with another obtained with the same numerical method but on a denser mesh is one of the most certain ways to judge how near the given solution is to the ultimate accuracy indicated by the converged sequence of solutions using successively refined meshes. Unfortunately, this measure has not been very practical for three-dimensional results because the computer resources (primarily memory) of even supercomputers (1- or 2-million words of real memory) do not allow refinement beyond the standard-size meshes of about 50,000 points. Recently, however, Control Data Corporation has built a Cyber 205 with 16M 64-bit words of memory and allowed me to compute some of the AGARD Working Group 7 test cases using meshes that contain double and even triple the number of cells in each of the three coordinate directions of the standard meshes used in our previous solutions for the Working Group.[1] On this machine, the present program[2] executes in 32-bit precision at an average rate of about 125 Mflops sustained over the entire computation.

Three dense-mesh solutions are presented here. The first was carried out for the ONERA M6 wing at conditions of $M_\infty = 0.84$ and $\alpha = 3.06$ deg and shows only small improvements in accuracy compared to our earlier standard-mesh solution. But the other two for the Dillner wing cases reveal much richer detail in the vortex shock-wave structure of these flowfields than was seen before. These computations confirm what aerodynamicists have recently claimed (based on wind tunnel measurements) must exist in real flowfields.[3,4]

ONERA M6 Wing: $M_\infty = 0.84$, $\alpha = 3.06$ deg

With double the number of cells in all the directions of the standard-mesh solution,[5] 192 cells are located around the chord, 40 on the span, and 40 outward from the wing to the far field 5 root chords away. The lift and drag computed on the coarsest grid ($48 \times 10 \times 10$) was 0.266 and 0.0167, respectively. The next level of refinement ($96 \times 20 \times 20$) produced 0.285 and 0.0113 and on the final grid ($192 \times 40 \times 40$) 0.283 and 0.0111. This indicates the very small overall change achieved with the last mesh refinement. Figure 1 shows that the suction peaks are nearer to the measured values, the pressure on the lower surface is in better agreement with the experiment, the shock waves are sharper, and the losses in the total pressure are more localized to the shocks. The isobars on the upper surface run together at the trailing corner of the tip exactly as in the standard-mesh solution, ratifying our earlier belief in the reality of this striking feature.[5]

70 deg Swept Dillner Delta Wing

The two solutions obtained with denser grids for subsonic and supersonic flows around the Dillner wing reveal flowfields of much more complex expansion and compression phenomena than the standard-mesh solutions do. In both cases, weak and local shock waves interact with the vortex over the wing. The solution computed for the subsonic case, $M_\infty = 0.7$ and $\alpha = 15$ deg, on a mesh of 160 cells around the semispan, 80 on the chord, and 48 from the wing outward to the far field, is presented in Fig. 2. The most striking feature—not seen in the standard-mesh solution, but clearly visible here in the isobars and total pressure contours—is the small shock wave situated between the vortex and the upper surface of the wing just outboard of the vortex core. From observations in wind tunnel experiments, Wendt[3] has recently suggested the existence of just such a shock wave. In overall comparison with the standard-mesh solution, the suction peak under the vortex is markedly stronger and produces the shock wave, the smearing of vorticity across the vortex sheet at the leading edge is significantly reduced, and the total pressure losses are confined to a tighter region centered on the core of the vortex. In the wake, the interaction of the leading- and trailing-edge vortices also is represented better.

Figure 3 displays the solution computed for the supersonic case, $M_\infty = 1.5$ and $\alpha = 15$ deg, on a mesh of 192 cells around the semispan, 96 on the chord, and 56 from the wing outward to the far field. The variation in pressure throughout this supersonic flowfield is not very great, but the coalescing of the Mach contours indicates the presence of a small shock wave intersecting the coiling vortex sheet just inboard of and above

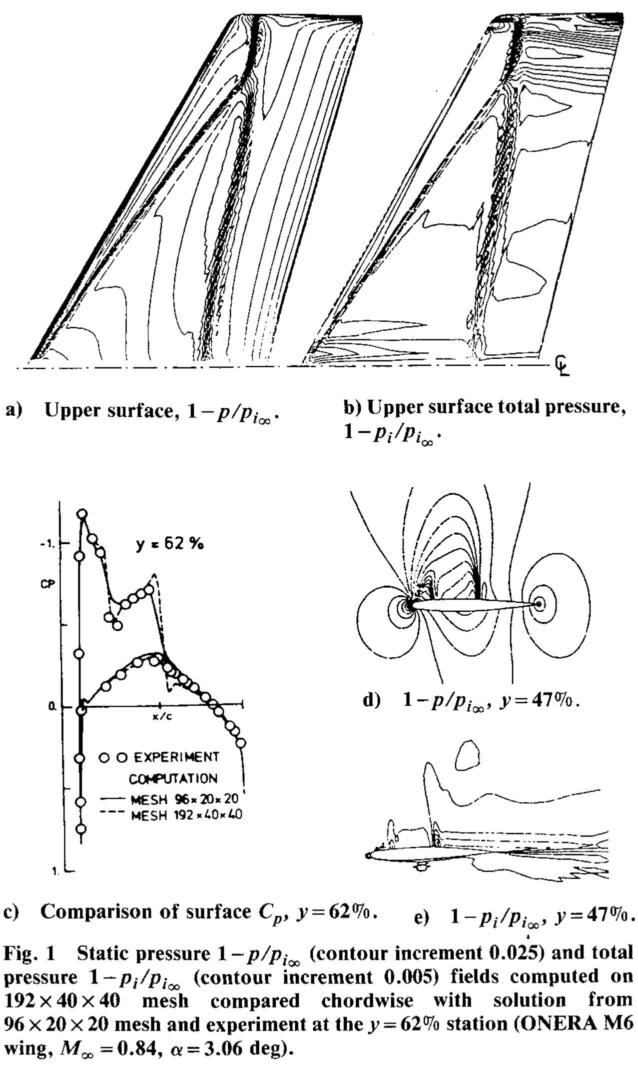

a) Upper surface, $1 - p/p_{i_\infty}$.

b) Upper surface total pressure, $1 - p_i/p_{i_\infty}$.

c) Comparison of surface C_p, $y = 62\%$.

d) $1 - p/p_{i_\infty}$, $y = 47\%$.

e) $1 - p_i/p_{i_\infty}$, $y = 47\%$.

Fig. 1 Static pressure $1 - p/p_{i_\infty}$ (contour increment 0.025) and total pressure $1 - p_i/p_{i_\infty}$ (contour increment 0.005) fields computed on $192 \times 40 \times 40$ mesh compared chordwise with solution from $96 \times 20 \times 20$ mesh and experiment at the $y = 62\%$ station (ONERA M6 wing, $M_\infty = 0.84$, $\alpha = 3.06$ deg).

Received Sept. 18, 1984; revision received Jan. 26, 1985.

*Research Scientist, Aerodynamics Department. Also, Adjunct Professor, Royal Institute of Technology, Stockholm. Member AIAA.

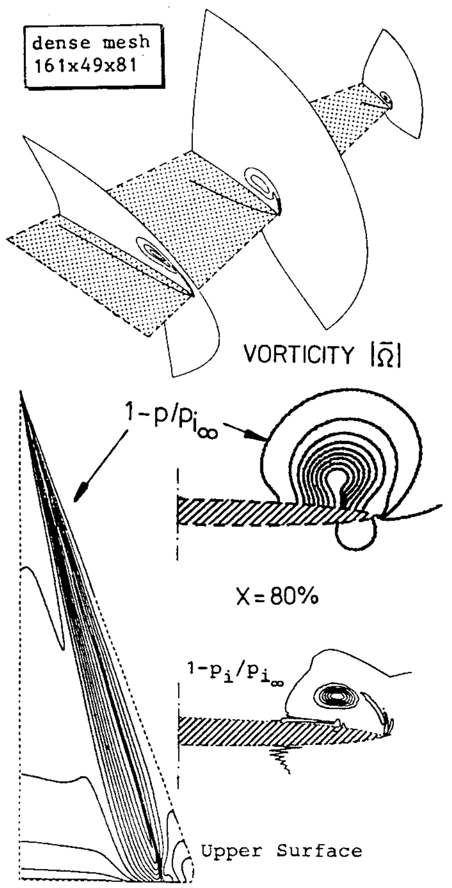

Fig. 2 Vorticity magnitude, static pressure $1-p/p_{i_\infty}$ (increment 0.05), and total pressure $1-p_i/p_{i_\infty}$ (increment 0.05) computed on an O-O mesh of $161\times 49\times 81$ points around the Dillner wing ($M_\infty=0.7$, $\alpha=15$ deg).

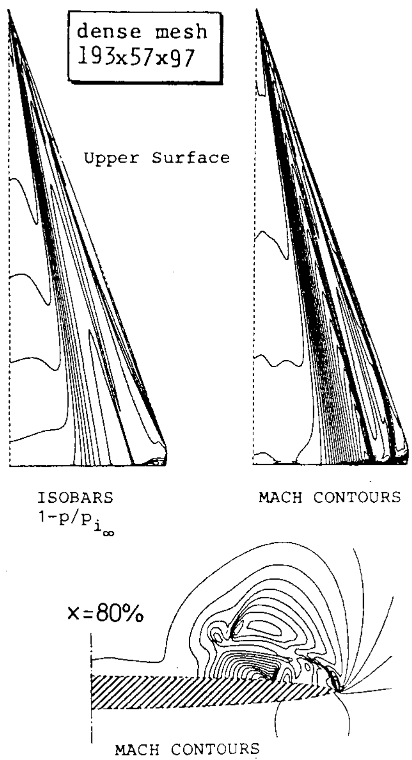

Fig. 3 Iso-Mach contours (increment 0.1) and isobars $1-p/p_{i_\infty}$ (increment 0.05) computed on an O-O mesh of $193\times 57\times 97$ points around the Dillner wing ($M_\infty=1.5$, $\alpha=15$ deg).

the core of the vortex. This feature of the flowfield is consistent with the experimental findings of Miller and Wood (see Fig. 12 in Ref. 4). Furthermore, we see in the Mach number contours on the upper surface at least two distinct shock waves between the suction peak and leading edge, forming a complex system of shocks and expansion waves being reflected from the apex to the trailing edge. Such phenomena should be expected because the flow, which is supersonic, has to turn abruptly where the vortex sheet leaves the leading edge. And accompanying these phenomena are heavy losses in total pressure.

Conclusions

The dense-mesh solutions presented here have shown that the flowfield around a trapezoidal wing like the M6 can be represented with reasonable accuracy on a standard-size mesh of, say, 50,000 grid points. But if the wing is one of low aspect ratio, like the Dillner delta wing, a much denser grid is required to capture the rich structure of the vortex flow interacting with the shock waves.

References

[1] *Test Cases for Inviscid Flow Field Methods*, Report of Fluid Dynamics Panel Working Group 07, AGARD-AR-211, Paris, May 1985.

[2] Rizzi, A., "Vector Coding the Finite-Volume Procedure for the CYBER 205," *Lecture Series Notes 1983-04*, von Kármán Institute, Brussels, 1983.

[3] Vorropoulos, G. and Wendt, J.F., "Laser Velocimetry Study of Compressibility Effects on the Flow Field of a Delta Wing," *Aerodynamics of Vortical Type Flows in Three Dimensions*, AGARD-CP-342, 1983, pp. 9-1–9-12.

[4] Miller, D.S. and Wood, R.M., "An Investigation of Wing Leading-Edge Vortices at Supersonic Speeds," AIAA Paper 83-1816, 1983.

[5] Rizzi, A.W. and Ericksson, L.-E., "Computation of Flow Around Wings Based on the Euler Equations," *Journal of Fluid Mechanics*, Vol. 148, Nov. 1984, pp. 45-71.

Boundary-Layer Thickness and Base Pressure

Mauri Tanner*
Institut für Theoretische Strömungsmechanik, DFVLR Göttingen, Federal Republic of Germany

Introduction

RESULTS from base pressure measurements at large boundary-layer thicknesses are rare and the present author had in vain sought such results in order to correlate with his own theory.[1,2] Recently, however, he discovered the measurements of Goecke,[3] which were performed on aft-facing steps in free flight. These experiments included relative boundary-layer thicknesses up to $\delta_2/d=0.85$, with δ_2 as boundary-layer momentum thickness and d as step height. It was found that the results of Goecke[3] could be well correlated with the theory.[1,2] Since this theory is relatively new and not widely known, its main outline is given first and then it will be used to correlate Goecke's results.

Received Sept. 20, 1984; revision received Nov. 9, 1984.

*Research Scientist.